

3D Strain Detection of a Support Implant for an Artificial Hip Joint

Using Finite Element Method and Genetic Algorithm

[†] Chika Maeda, [†] Syoji Kobashi, [‡] Nao Shibamura, [†] Katsuya Kondo and [†] Yutaka Hata

[†] Graduate School of Engineering, University of Hyogo

[‡] Kobe Kaisei Hospital

E-mail maeda@comp.eng.himeji-tech.ac.jp

Abstract

A form of a support implant used in revision total hip arthroplasty (THA) should be diagnosed periodically because it may be distorted or broken. This paper proposes a new method that estimates the strength of stress on the support implant using finite element method (FEM) and genetic algorithm (GA). 3D sectional images of the support implant in vivo are acquired from multidetector-row computed tomography (MDCT) devices. The proposed method searches for a model whose shape is same as the support implant in MDCT images using GA. The database consists of many parts of the support implant that are generated by FEM with various patterns of strain. Direction and strength of the stress are estimated from the searched model. As a result of the proposed method applying to simulated MDCT images of horseshoe-shaped phantoms, the proposed method found the correct model. Also, the method detected the strain within the error of $1.03 \pm 0.38\text{mm}$ and $33.0 \pm 12.3\text{N}$. Additionally, we applied the method to MDCT images of 2 patients after THA. The results showed that the direction and the strength of the stress were successfully estimated.

1. Introduction

Total hip arthroplasty (THA) patients who are induced pain by accidental rotation or displacement should revise the component. Revision THA is an operation to replace the broken artificial hip joint with a new artificial hip joint [1]. In this operation, a support implant is used to reconstruct the artificial hip joint on the acetabulum. The artificial hip joints and the support implant might be deformed or be broken by strong stress or with age. Because the deformed or broken implant can cause serious problems for patients, we

should periodically diagnose the shape of the implant after THA.

There are conventional methods for diagnosing the support implant [1]-[3]. Tanaka *et al.* proposed a new method that physicians visually evaluate the shape of the postoperative implant with X-ray images [1]. However, it is impossible to obtain the 3D shape of the implant because the X-ray image is a 2D projection image. Also, quality of diagnosis depends on physicians or X-ray images. Therefore, another method that quantitatively evaluates the implant based on 3D form should be studied. We have previously developed a method using a multidetector-row computed tomography (MDCT) scanner [2][3]. The method calculates distortion angles between a 2D projection image of a 3D geometric model and a 2D projection image of the support implant in MDCT images by finding corresponding characteristic points between them. Using MDCT images, we could make a 2D projection image of the support implant from arbitrary viewpoint. However, the method could not calculate the 3D distortion of the support implant. In addition, the method avoids any mention of strength and direction of the stress on the support implant.

In general, detection of strain can be achieved by finding characteristic points of an object of interest, and measuring the distance or the angle among the characterizing points. However, in case of 3D objects, it is a hard work to recognize the 3D shape and to find characteristic points. Finite element method (FEM) is an effective approach to analyze strain by a given stress. FEM has been applied to clinical researches [4][5].

Our objective is to propose a new method to detect the 3D strain of the support implant and to estimate the strength and the direction of the stress. To detect the strain of the support implant, our method finds a 3D model whose shape is same as the support implant in MDCT images from a database.

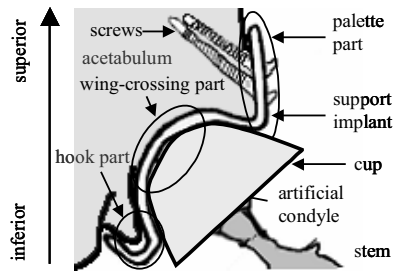


Figure 1. Structure of the artificial hip joint.

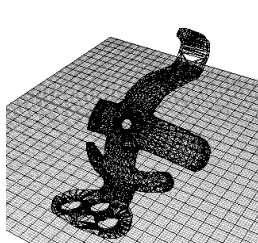


Figure 2. 3D visualization of the 3D geometric model of the support implant.

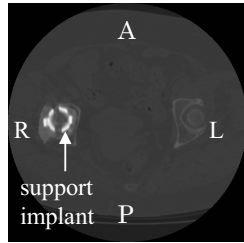


Figure 3. An example of MDCT image. (A; anterior, P; posterior, R; right, L; left)

The database consists of many parts of the support implant that are stimulatory generated by FEM with various patterns and stress for a 3D geometric model. So, searching the most fitted model from database is performed with genetic algorithm (GA).

2. Materials

The structure of an artificial hip joint is illustrated in Figure 1. Acetabular bone loss is filled with cancellous morselized bone, and is associated with cemented or noncemented acetabular components. The support implant is placed on the acetabulum and is bolted by screws. The cup made of polyethylene is put on the support implant. The artificial condyle and the stem are embedded in the cup. In this study, we used KT plate (Japan Medical Materials, Ltd, Osaka) as the support implant. The 3D geometric model of the support implant was given by parasolid format. Figure 2 shows the 3D visualization of the 3D geometric model.

We acquired MDCT images with two MDCT scanners (Aquilion; Toshiba, Tokyo, and Light Speed Ultra 16; GE Medical Systems, Milwaukee, WI). An example of MDCT image is shown in Figure 3. As shown in this image, although there are artifacts caused by metal, there are differences of CT values between the implants and the artifacts. Also, we could not find

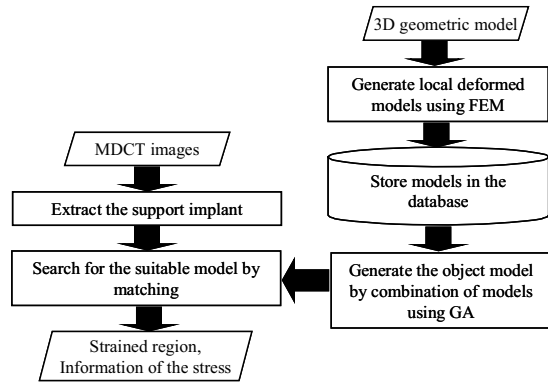


Figure 4. Outline of the proposed method.

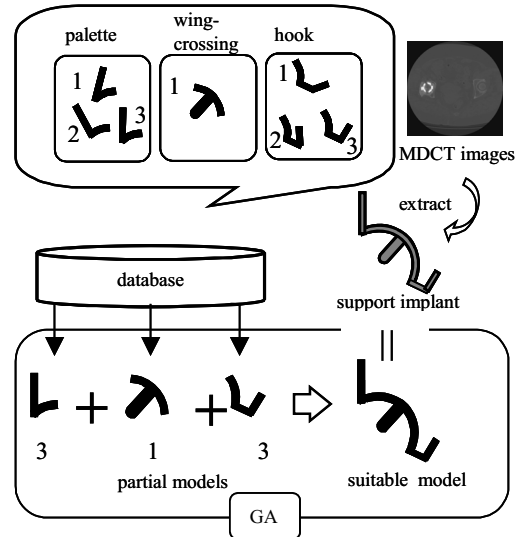


Figure 5. The illustration of outline of proposed method.

any differences between an MDCT images taken by the one scanner and that taken by the other scanner.

3. 3D strain detection using finite element method

Our method finds a 3D model whose shape is fitted to the support implant in MDCT images. Outline of the proposed method is shown in Figure 5. In preliminary, we construct a database that consists of a lot of partial models generated by FEM. For given MDCT images, the method segments the region of support implant using fuzzy object model, which is a method we have previously developed [2]. Next, the method finds the

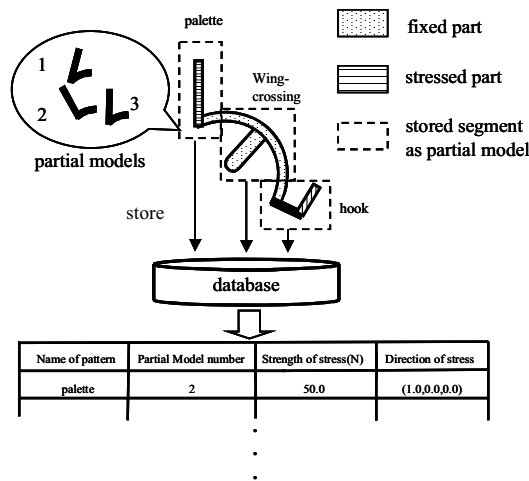


Figure 6. The illustration of generating partial models and the database.

best combination of partial models, in which the combination is the most similar the segmented support implant based on GA.

3.1 Construction of a database that has partial models using FEM

Support implant can be segmented into three parts; palette part, wing-crossing part and hook part, as illustrated in Figure 1. Through our clinical experiments and knowledge, we know that most of strains are occurred at the palette part or the hook part. It will be because of the shape of the support implant and the setting position on acetabulum.

Therefore, we construct a database using three kinds of parts; palette part, wing-crossing part and hook part as follows. For each part, we generate many patterns with changing the strength of stress using FEM. In FEM simulation, we fix the wing-crossing part when straining the palette part or the hook part. The number of strained patterns of the palette part and hook part are N_d and N_h , respectively. In summary, the database consists of three kinds of parts; a datum of a pattern has following items; 1) name of pattern (palette, wing-crossing or hook), 2) partial model number, 3) strength of stress, 4) direction of stress, and 5) 3D geometric model generated by FEM with given strength and direction of stress. An example of database is shown in Figure 6.

3.2 Searching for the suitable model using genetic algorithm

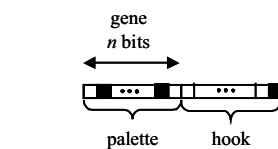


Figure 7. Chromosome encoding.

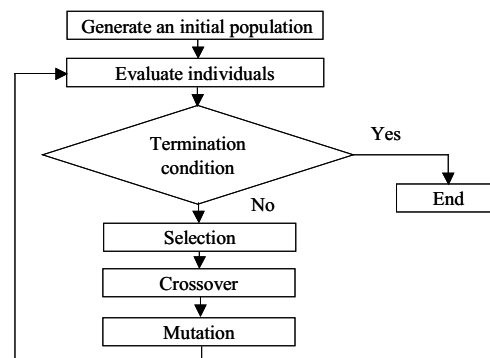


Figure 8. Flow chart of GA.

Our database has a large number of the partial models. So, we employ GA in order to searching for a combination of partial models that fit to the support implant in MDCT images.

We encode a combination of partial models as a list of bits. As illustrated in Figure 7, a chromosome is composed of two parts. Each part represents the partial model number of the palette part or hook part. And it is composed of n bit. Thus, one chromosome consists of $2n$ bits.

3.2.1 Combining models using genetic algorithm.

We generate a population of chromosomes. The population is evolved with respect to three rules: 1) the selection/reproduction that evaluate the performance of each individual and select only the good one; 2) the mutation which randomly modifies some bits of the chromosome and which is responsible for the search space exploration; and 3) the crossover which swaps the genetic material between some elected couples of chromosomes. In our method, chromosomes are selected by roulette wheel selection.

Flow chart of GA is shown in Figure 8. If the specified fitness (we call the value of the objective function 'fitness' in this paper) will be obtained, the object model that has the best fitness is defined as the suitable model. We obtain the strength and the direction of the support implant by referring partial models.

3.2.2 Objective function of genetic algorithm.

In our system, objective function of GA evaluates whether the combination given by the chromosome fits

to the support implant in MDCT images. Consider a chromosome whose number of partial model is x_d , x_w , and x_h . To evaluate each part of chromosome, at first, we construct a 3D geometric model by combining the given partial models. The constructed model is transformed into voxel data whose value is zero and one. Zero means that the voxel is outside of the constructed model, and one means that the voxel is inside of the constructed model. We perform image matching between the constructed 3D geometric model and the support implant in MDCT images. Matching score is

$$\mu = \frac{\sum_{x,y,z} G(x,y,z) \times H(x,y,z)}{\sum_{x,y,z} G(x,y,z)}, \quad (1)$$

where $G(x,y,z)$ means a value stored at voxel (x,y,z) in the constructed model, and $H(x,y,z)$ means a value stored at voxel (x,y,z) in the MDCT images. The support implant voxels in MDCT images are allocated weight value 1.0. 26-neighborhood of these voxels are allocated weight value based on gaussian distribution.

4. Experimental Results

In this study, FEM was performed with ANSYS 9.0. To evaluate the performance of the proposed method, we applied our method to simulated MDCT images and the MDCT images of 2 THA patients.

4.1 Experiments on simulated MDCT images of phantoms

To evaluate the accuracy of the proposed method, we applied a horseshoe-shaped phantom. 3D visualization of the horseshoe-shaped phantom is shown in Figure 9. Material setting of the horseshoe-shaped phantom was titanium same as the support

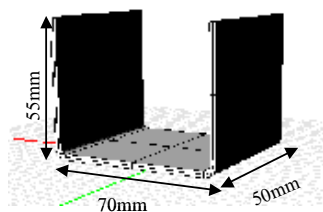


Figure 9. 3D visualization of horseshoe-shaped phantom.

implant. Besides, thickness of the phantom was 2.5 mm which same as the support implant.

To construct database, we applied the stress to side surfaces of the phantom. Also, we defined the bottom surface as the fixed part. The strength of the applied stress was changed from 0.0 to 275.0 N every 27.5 N. The number of segment patterns was 11. The number of partial models was 3. The voxel size of simulated MDCT images set as $0.5 \times 0.5 \times 0.5 \text{ mm}^3$ as similar as MDCT images. Intensity of phantom voxels was 4000 hounsfield unit (HU) which similar value as that of titanium. Also, These images were convoluted by a gaussian function (FWHM; full width half maximum = 2 voxels) in order to blur the contour of metal region. Examples of the simulated MDCT images of the horseshoe-shaped phantom are shown in Figure 10. The horseshoe-shaped phantom region was extracted by thresholding algorithm. Parameters of GA were follows; population was 5, one-point crossover rate was 0.85, and mutation rate was 0.1. If μ exceeded 0.9 or the generation number became 30, termination condition will be fulfilled. We tried the proposed method 5 times with different initial populations. The highest fitness values on each generation are shown in Figure 11. The final solution was obtained an average of 8.8 generations. Examples of the constructed model on generated each generation of phantom 1 are shown in Figure 12. Suitable models of phantom 2 and phantom 3 are shown in Figure 13. Results of applying the proposed method to three kinds of the phantoms are tabulated in Table 1. In this table, error of shape means maximum Euclidean distance between the constructed model on the final generation and the support implant in MDCT images. We are considering that proposed method can be applied to simulated MDCT images within the error of $1.03 \pm 0.38 \text{ mm}$ and $33.0 \pm 12.3 \text{ N}$. A main cause for the error is the error by voxelization of the suitable model. In addition, the contour of the object model region was blurring in simulated MDCT images.



Figure 10. Examples of the simulated MDCT images of the horseshoe-shaped phantom.

4.2 Experiments on MDCT images of 2 patients

We have applied the proposed system to MDCT images taken from 2 subjects (59 and 73 years, 23 and 26 months after THA). The MDCT images used in this study were acquired with a matrix of 512×512 , a pixel size of $0.637 \times 0.637 \text{ mm}^2$ or $0.653 \times 0.653 \text{ mm}^2$, a slice

thickness of 0.5 mm, a tube current of 300 mA and a tube voltage of 120 kV. For each subject, over 460 slices were taken so that the whole implant was covered. The extracted implant region by thresholding and labeling is shown in Figure 14. As shown in the images, the support implant region was well segmented. Next, to construct database, we performed FEM with changing the strength of stress from -283.0 to 283.0 N

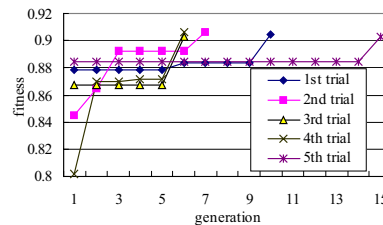


Figure 11. Transition of the fitness (phantom1, 5 times trial).

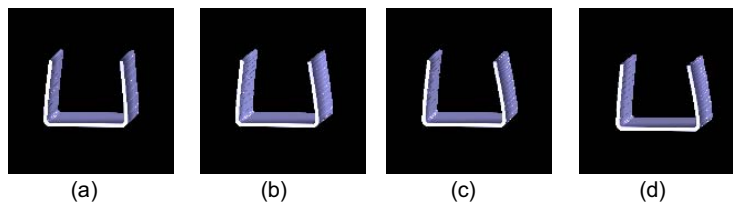


Figure 12. Generated suitable models of phantom 1 (in 4th trial). (a) Model of generation 1. (b) Model of generation 4. (c) Model of generation 6. (d) Phantom 1.

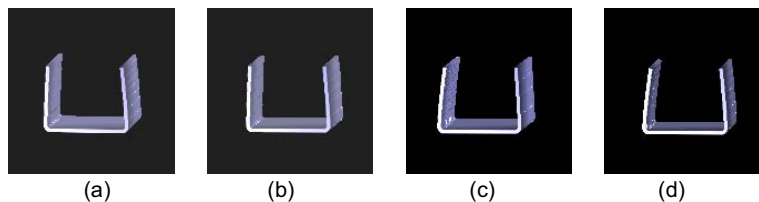


Figure 13. Phantoms and suitable models. (a) Phantom 2. (b) Suitable model of phantom 2. (c) Phantom 3. (d) Suitable model of phantom 3.

Table 1. Error of the estimated suitable model (5 times trial).

Phantom	Shape (mm)			Stress (N)		
	Truth value	Estimated value (mean±SD)	Error (mean±SD)	Truth value	Estimated value (mean±SD)	Error (mean±SD)
1	7.79	6.76±0.38	1.03±0.38	247.5	231±15.1	16.5±15.1
2	3.48	2.96±0.47	0.52±0.47	110.0	77±12.3	33.0±12.3
3	6.08	5.22±0.01	0.86±0.01	192.5	165±0.0	27.5±0.0

every 28.3 N for each of palette part and hook part. Thus, we generated 20 patterns for each part.

Parameters of GA were follows; population was 5, two-point crossover rate was 0.85, and mutation rate was 0.1. If μ exceeded 0.8 or the generation number became 30, termination condition will be fulfilled. We applied the proposed method 5 times with changing initial population. Fitness on each generation is shown

in Figure 15. The best solution was obtained an average of 19.8 generations. Results of applying the proposed method to 2 patients were tabulated in Table 2. In this table, we were considering that proposed method could be applied to patient data. Color chart that represents Euclidean distance between the suitable model and the support implant in MDCT images is shown in Figure 16. The color chart of the stress was shown in Figure 17.

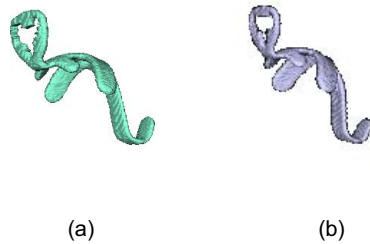


Figure 14. The extracted support implant. (a) Patient A. (b) Patient B.

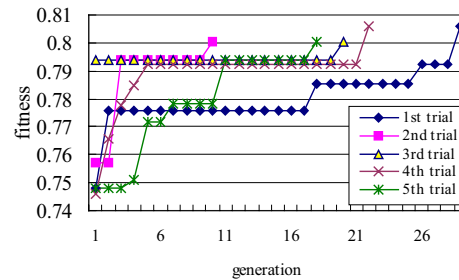


Figure 15. Transition of the fitness (patient A, 5 times trial).

Table 2. Strength and direction of the stress of patients (mean±SD)(5 times trial).

Patient	Strength (N)		Unit vector of direction (x,y,z)	
	Palette	Hook	Palette	Hook
A	28.3±14.1	28.3±14.1	(1.0, 0.0, 0.0)	(0.5, 0, 0.5)
B	56.6±14.1	28.3±14.1	(1.0, 0.0, 0.0)	(0.5, 0, 0.5)



Figure 16. Color chart of Matching results that represents Euclidean distance between the suitable model and the support implant in MDCT images. (a) Patient A. (b) Patient B.

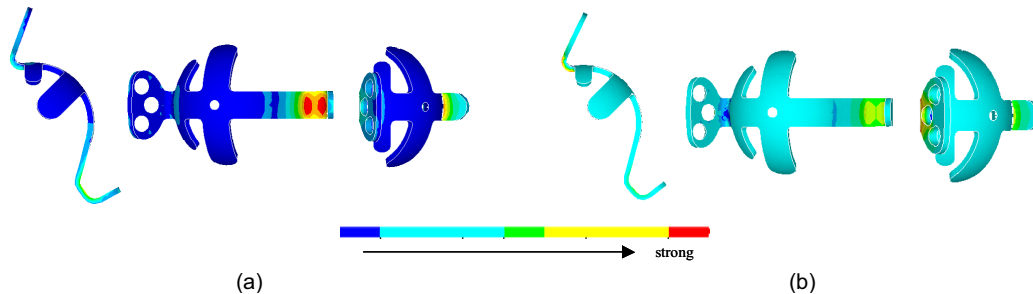


Figure 17. Color chart of the stress. (a) Patient A. (b) Patient B.

In this figure, the more color of the part becomes red, the stronger stress was loaded. From this figure, we could confirm a distribution of the stress on the support implant *in vivo*.

5. Conclusion

In this paper, we have proposed the strain detection method for a support implant using FEM and GA. The proposed method detects the strain by finding the model whose shape fits to the support implant in MDCT images. Our proposed method can detect the strain of the support implant *in vivo*. Additionally, the strength and the direction of the stress on the support implant can be calculated. So, this method can strongly support the postoperative periodical prognosis.

To evaluate the performance of the proposed method, we have done two types of experiments; computer simulation using phantom and subject experiments. The first experiment for simple objects showed that our method detected the strain within the error of 1.03 ± 0.38 mm and 33.0 ± 12.3 N. In the second experiment for 2 patients after THA, the proposed method detected the strain region and the strength and direction of the stress that had been strained to the support implant successfully. In the future, we will apply for another implants, for example, femoral component and tibia tray. Also, we should evaluate the accuracy of estimating the strength of stress that was loaded to the support implant *in vivo*.

Acknowledgement

The authors thank to Hakubikai Imaging Support Center and Ishikawa Hospital that provided MDCT images. This work was supported in part by Ishikawa Hospital Grant, and Berkeley Initiative in Soft Computing (BISC) Program of UC Berkeley.

References

- [1] C. Tanaka, S. Jitsuhiko, M. Ikenaga and T. Makoto, "Acetablar Reconstruction Using a Kerboul-Type Acetablar Reinforcement Device and Hydroxyapatite Granules," *The Journal of Arthroplasty*, 2003, vol.18, no.6, pp.719-725.
- [2] C. Maeda, S. Kobashi, K. Kondo and Y. Hata, "Fuzzy Object Model-based Image Segmentation for *in vivo* Evaluation of Support Implant of Artificial Hip Joint," *Soft Computing and Intelligent Systems*, 2004, CD-ROM.
- [3] N. Shibanuma, S. Kobashi, C. Maeda, Y. Hata and M. Kurosaka, "Distortion Detection of a Support Implant for Artificial Hip Joint Using Multiscale Matching Algorithm,"

International Conference on Systems, Man and Cybernetics, 2005, (in press).

[4] Y. Chi, D. Choi, J. Kim, G. Cho and Y. Yoon, "The Application of 3-D X-ray Microtomography with FEM Analysis for Trabecular Bone/Cement Interface," *Nuclear Science Symposium Conference Record*, 2003, vol.4, pp.3009-3013.

[5] K. Shaw, M.D. Nowak, C. Lewis and J.D. Enderle, "Development of a Tibial Slider to Evaluate and Validate a Finite Element Model for Friction in Total Knee Implants," *Proceedings of the IEEE 26th Annual Northeast Bioengineering Conference*, 2000, pp.13-14.